Thermal conductivity of opals and related composites

J. D. Albrecht
Naval Research Laboratory, Washington, DC 20375

P. A. Knipp
Christopher Newport University, Newport News, Virginia 23606

T. L. Reinecke
Naval Research Laboratory, Washington, DC 20375

(Received 6 October 2000; published 15 March 2001)

The thermal current flow through periodic composites and the corresponding effective thermal conductivities are studied within a continuum approach. We formulate a boundary-integral method for calculating the thermal conductivity of structures with two- and three-dimensional periodic lattices. Explicit results are given for lattices involving overlapping features and contact is made with the Maxwell approximation for simple porous media. As a particular example detailed calculations are made for the thermal conductivities of media in the synthetic opal class of composites. We consider opals that are comprised of overlapping spheres arrayed in face-centered-cubic lattices and inverse opals that are formed by filling the interconnected pores of opal lattices.

DOI: 10.1103/PhysRevB.63.134303 PACS number(s): 66.70.+f, 42.70.Qs, 66.90.+r

I. INTRODUCTION

Recent advances in fabrication techniques are providing the opportunity to engineer the properties of materials by varying the underlying structure on several length scales including the mesoscopic scale. Such materials are being studied both for their basic properties as well as for a range of technological opportunities. The thermal conductivity of these systems is of current interest in connection with cooling applications. The quality of a material for thermoelectric cooling is given by its thermoelectric figure of merit $Z=\sigma_o S^2/\kappa$ where σ_o is the electrical conductivity S the Seebeck coefficient, and κ the total thermal conductivity. Thus materials with relatively low thermal conductivities are sought for thermoelectric applications. Conversely in situations where the cooling occurs directly by a heat current a large thermal conductivity is sought. Composites offer the possibility of modifying thermal transport of a host material in both of these directions.

Materials of interest with mesoscopic structuring include synthetic opals as well as a number of more complex systems such as porous Bi films. Synthetic opals are typically formed from a periodic array of SiO_2 spheres having sizes ranging from tens of nanometers to microns.[1,2] In opals, the spheres are replaced with a variety of materials and are sintered to make their spheres overlap at the ''necks.'' In addition ''inverse opals'' are formed by filling the voids between the spheres with another material and removing the material in the spheres. Opals and inverse opals have periodicities on the scale of the original spheres. The thermal optical and electrical properties of opals are of current interest in connection with issues ranging from thermoelectric materials to photon band gap systems. In the present context they also provide a class of well defined systems whose properties reflect a broader range of nonperiodic composites. Here we study the thermal conductivities of opals to understand better the role of structuring on their overall thermal conductivity.

We use a continuum description in which the thermal conductivity of each region of the composite is represented by its bulk thermal conductivity. This approach is appropriate for systems in which the thermal phonon mean free path λ is smaller than the typical structural size $\lambda \ll a$. For SiO_2 we estimate a low temperature thermal phonon mean free path of $\lesssim 1$ nm.[3] Among typical materials of interest in thermoelectrics we estimate room temperature thermal phonon mean free paths of 7.5 nm for Bi and 17.5 nm for PbTe.[4] The continuum approach is appropriate for opal sizes greater than these values. The intent of this work is to address the role of structuring on thermal conductivity. Interface scattering and changes in phonon dispersions are also of interest in the thermal conductivities of composites. These effects could be included in the present approach by interface resistances.[5,6] They are not yet well understood, however, and are material dependent and they will not be addressed here.

The thermal conductivity of a composite within a continuum description can be given by a simple Maxwell-Garnett or Clausius-Mossotti approach.[7] For example, for systems of spherical voids ($d=3$) or infinite cylindrical voids ($d=2$) in a material of thermal conductivity κ_o this gives for the effective conductivity

$$\kappa_{eff}=\frac{(1-p)\kappa_o}{1+p/(d-1)}, \tag{1}$$

where p is the fractional volume of the voids often called the ''porosity.'' This approach represents the geometry of the system in only an approximate way and is accurate only when either the fractional volume of one material or the difference in the conductivities of the two systems is small. In general its accuracy is difficult to assess. It also does not

represent well the effects of geometry such as the ordered structure of the opal. In recent work a continuum description has been used to study analytical bounds on the thermal conductivity of composites in terms of its constituent parts.[8] In other recent work the thermal conductivity of opals in the ballistic limit in which $\lambda \gg a$ was examined[9] which gives a treatment appropriate for small sizes and is complementary to that given here.

Here we solve for the steady-state heat current resulting from an external thermal gradient in two- and three-dimensional systems representing opals. We use Green's-function techniques to transform the problem to a form in which efficient boundary element discretization can be used. Typically this transforms a differential equation in d dimensions to one in $(d-1)$ dimensions.[10,11] In the present case we develop a cell periodic form of the boundary element method to treat the opals.

The techniques that we develop here can also be used to describe other physical properties of ordered composites. For example the so-called photon band-gap systems have refractive indexes that are modulated periodically and can exhibit gaps in their photon spectrum analogous to the electronic states of solids. The equations governing the electromagnetic behavior of these systems are formally equivalent to the heat transport problem studied here and the techniques developed here can be used to treat that problem.[12]

In Sec. II we give a boundary-integral method for calculating the thermal current in a periodic composite. Results for two-dimensional lattices are given in Sec. III and three-dimensional lattice calculations are given in Sec. IV.

II. FORMALISM

In this section a formalism based on a continuum approach is given for calculating the flow of heat current through periodic composites. We consider structures composed of three-dimensional lattices (e.g., opals) and of two-dimensional lattices with features that extend infinitely in the third direction. The insets of Fig. 1 give examples of such two-dimensional lattices. The systems are composed of homogeneous regions that describe the unit cell in a periodic array as indicated by the dotted lines in Fig. 1. The present method is general for composites containing any number of component materials as long as the composite has a periodic lattice. A constant value for the local thermal conductivity characterizes each region consistent with the continuum approach. For simplicity we take these local thermal conductivities to be isotropic and independent of temperature. We calculate the thermal current flow through a composite without internal heat sources in response to an externally applied temperature gradient and determine the effective conductivity of the composite from the calculated current.

The periodic composites are described by unit cells composed of regions with thermal conductivities labeled κ_i. For systems with no internal heat sources and with steady-state current density $\mathbf{J}$ the quantity $\nabla \cdot \mathbf{J}$ $(=\nabla \cdot [\kappa_i \mathbf{F}] = \kappa_i \nabla \cdot \mathbf{F})$ vanishes inside all regions. Here a thermal field $\mathbf{F}$ is given from the temperature by $\mathbf{F} = -\nabla T$. It follows that the temperature satisfies Laplace's equation $\nabla^2 T = 0$, in all regions

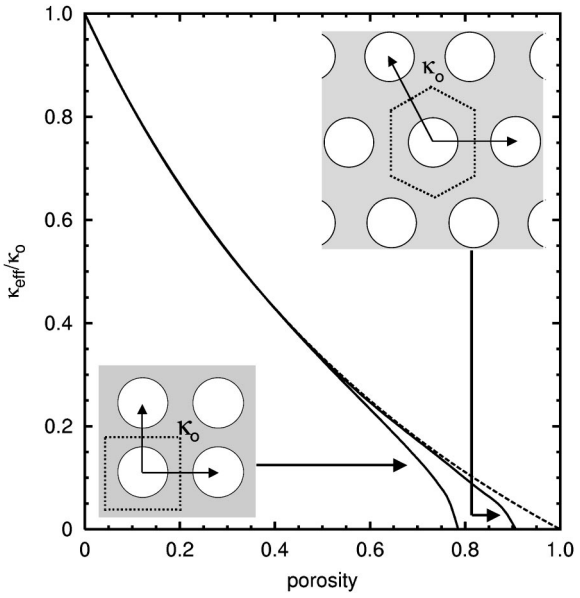

FIG. 1. Thermal conductivities as functions of porosity for square and hexagonal two-dimensional lattices. The dashed curve is the Maxwell model. Schematic lattice geometries are shown in the insets.

and is continuous across boundaries. In addition to the partial differential equation we must specify boundary conditions for the thermal current crossing the interfaces between the regions. The continuity of the thermal current normal to the interfaces and the continuity of the temperature provide the physically appropriate boundary conditions. For many of the structures described here one of the two material regions is void resulting in vanishing thermal currents inside. The boundary conditions are appropriate in this case because the current does not penetrate the void regions.

The integral equation method we use is based upon calculating the current density arising from an external temperature gradient $\mathbf{F}_o$. An external field leads to an inhomogeneous integral equation for the total thermal field and hence the current, throughout the composite. By applying an external field a composite conductivity calculation can be made that is independent of terminal surfaces or heat source placement. Here we treat isotropic lattices but the formalism is general and also can be used in low-symmetry directions in anisotropic systems. In the next section we demonstrate the flexibility of this technique by treating a low-symmetry direction.

In general the temperature can be written in terms of a Green's function as an integral equation over all of the boundaries in the composite S. The expression for the temperature is

$$T(\mathbf{r}) = -\mathbf{F}_o \cdot \mathbf{r} + \int_S \sigma(\mathbf{s}) g(\mathbf{r}-\mathbf{s}) d\mathbf{s}, \tag{2}$$

where $g(\mathbf{r})$ is the Green's function and equals $-2\ln|\mathbf{r}|$ or $|\mathbf{r}|^{-1}$ for two- or three-dimensional lattices, respectively. Below we solve for σ, a function defined only on the boundaries between regions by applying boundary conditions. To

see the role played by the function σ it is useful to note the analogy between this problem and an inhomogeneous system of dielectrics in an electric field.[11] In the case of the dielectrics σ represents the surface charge densities which give rise to the fields. In our case the function σ gives rise to the temperature gradients.

The integral over all interfacial boundaries S between the components of the periodic composite can be reduced to an integral over all boundaries inside a unit cell $\tilde{S}$, by defining a cell-periodic Green's function $\tilde{g}$. The integral of Eq. (2) then is replaced using

$$\int_S \sigma(\mathbf{s}) g(\mathbf{r}-\mathbf{s}) d\mathbf{s} = \int_{\tilde{S}} \sigma(\mathbf{s}) \tilde{g}(\mathbf{r}-\mathbf{s}) d\mathbf{s}, \tag{3}$$

where

$$\tilde{g}(\mathbf{r}) = \sum_{\mathbf{t}} g(\mathbf{r}-\mathbf{t}) = \frac{4\pi}{\Omega} \sum_{\mathbf{G}\neq\mathbf{0}} \frac{e^{i\mathbf{G}\cdot\mathbf{r}}}{G^2}. \tag{4}$$

The summation in the first form in Eq. (4) is over all lattice translations $\mathbf{t}$ or equivalently over all reciprocal-lattice vectors $\mathbf{G}$ as shown in the second form. The volume or area of the primitive cell is Ω. The sum in Eq. (4) converges slowly in real space because the Green's functions have long-range character. Owing to the strong singularity at the origin the reciprocal space sum also converges slowly.

Rapidly converging series expressions for $\tilde{g}$ are obtained by straightforward extension of Ewald summation techniques.[13] The slowly converging summation is reformulated by introducing a free parameter η. Without loss of generality we rewrite the lattice sum for $\tilde{g}$ by adding to the series equal and opposite Gaussian ''sources'' at all equivalent lattice sites. Controlling the Gaussian widths by η we rewrite the series in Eq. (4) as

$$\tilde{g}(\mathbf{r}) = \sum_{\mathbf{t}} \left\{ \left(g(\mathbf{r}-\mathbf{t}) - \left(\frac{\eta}{\pi}\right)^{\mu} \int e^{-\eta x^2} g(\mathbf{r}-\mathbf{t}-\mathbf{x}) d\mathbf{x} \right) + \left[\left(\frac{\eta}{\pi}\right)^{\mu} \int e^{-\eta x^2} g(\mathbf{r}-\mathbf{t}-\mathbf{x}) d\mathbf{x} \right] \right\} \tag{5}$$

with $\mu = 1$ and $\frac{3}{2}$ giving proper normalizations for two-dimensional (2D) and three-dimensional (3D) lattice sums, respectively. The first two terms are evaluated in real space and the term in brackets is evaluated in reciprocal space. The result is two quickly converging sums controlled by η. After simplification[14] the Ewald summation procedure yields the following expressions for the lattice Green's functions:

$$\tilde{g}(\mathbf{r}) = \frac{4\pi}{\Omega} \sum_{\mathbf{G}\neq\mathbf{0}} \frac{e^{i\mathbf{G}\cdot\mathbf{r}}}{G^2} e^{-G^2/4\eta} + \begin{cases} \sum_{\mathbf{t}} E_1(\eta|\mathbf{r}-\mathbf{t}|^2) & (2\mathrm{D}) \\ \sum_{\mathbf{t}} \dfrac{\mathrm{erfc}(\sqrt{\eta}|\mathbf{r}-\mathbf{t}|)}{|\mathbf{r}-\mathbf{t}|} & (3\mathrm{D}) \end{cases}. \tag{6}$$

The free parameter η is tuned in each case so that the real-space and reciprocal space summations converge within a similar number of terms. A typical value for η is the square of the reciprocal-lattice constant. The number of terms required for convergence is lattice dependent and is greater for three-dimensional lattices.

To set up the integral equation we evaluate the thermal field, $\mathbf{F} = -\nabla T$ at boundary points $\mathbf{r}_s$ between the regions. The thermal fields approaching the boundary from inside and outside a homogeneous region are given by

$$\mathbf{F}_{in/out}(\mathbf{r}_s) = \mathbf{F}_o \mp 2\pi\sigma(\mathbf{r}_s)\hat{\mathbf{n}}_{\mathbf{r}_s} - \int_{\tilde{S}} \sigma(\mathbf{s})[\nabla_{\mathbf{r}} \tilde{g}(\mathbf{r}_s-\mathbf{s})] d\mathbf{s}, \tag{7}$$

where $\hat{\mathbf{n}}_{\mathbf{r}_s}$ is the unit normal vector at $\mathbf{r}_s$ and the upper sign corresponds to the interior. The final integral equation results from the current continuity boundary condition $\mathbf{J}_{in}\cdot\hat{\mathbf{n}}_{\mathbf{r}_s} = \mathbf{J}_{out}\cdot\hat{\mathbf{n}}_{\mathbf{r}_s}$. Substituting the thermal field expression of Eq. (7) into $(\kappa_{in}\mathbf{F}_{in} - \kappa_{out}\mathbf{F}_{out})\cdot\hat{\mathbf{n}}_{\mathbf{r}_s} = \mathbf{0}$ results in an integral equation for σ that can be simplified by collecting terms to give

$$\int_{\tilde{S}} \sigma(\mathbf{s})[\hat{\mathbf{n}}_{\mathbf{r}_s}\cdot\nabla_{\mathbf{r}}\tilde{g}(\mathbf{r}_s-\mathbf{s})] d\mathbf{s} + 2\pi\sigma(\mathbf{r}_s)\frac{(\kappa_{in}+\kappa_{out})}{(\kappa_{in}-\kappa_{out})} = \mathbf{F}_o\cdot\hat{\mathbf{n}}_{\mathbf{r}_s}. \tag{8}$$

Equation (8) is the central result of the boundary-integral formalism for these periodic systems. Upon discretization of the boundary Eq. (8) forms a matrix inversion problem to be solved for $\sigma(\mathbf{r}_s)$. Interestingly, for two-dimensional lattices the integrand of Eq. (8) does not require the evaluation of the exponential integral in Eq. (6) because of its simple radial dependence. However, for three-dimensional lattices evaluating the complementary error function cannot be avoided because of the additional $|\mathbf{r}|^{-1}$ dependence in the real-space sum.

The function σ on the boundary completely determines the current and conductivity. Given $\sigma(\mathbf{r}_s)$ the current density at an arbitrary nonboundary point $\mathbf{r}$ is reduced to evaluating the local thermal field using the following expression:

$$\mathbf{J}(\mathbf{r}) = \kappa(\mathbf{r})\mathbf{F}_o - \kappa(\mathbf{r}) \int_{\tilde{S}} \sigma(\mathbf{s})[\nabla_{\mathbf{r}}\tilde{g}(\mathbf{r}-\mathbf{s})] d\mathbf{s}. \tag{9}$$

An effective thermal conductivity is calculated by integrating the thermal current crossing an infinite plane. Taking the plane to be perpendicular to the driving field the integral over the plane maps to integrating the current component directed along the external field over the unit-cell volume in periodic composites. We define κ_{eff} by

$$\kappa_{eff} \equiv \frac{1}{\Omega|\mathbf{F}_o|} \int_{\Omega} \hat{\mathbf{f}}\cdot\mathbf{J}(\mathbf{r}) d\mathbf{r}, \tag{10}$$

where $\hat{\mathbf{f}}$ is the direction of the applied field and Ω is the cell volume (or area for two-dimensional lattices). In general the conductivity is a tensor quantity. For anisotropic systems the tensor components are resolved be applying the external field

along the principal axes. It is convenient to display κ_{eff} compared to the bulk conductivity of the material composing the majority of the composite. We denote this conductivity by κ_o in the following.

III. TWO-DIMENSIONAL SYSTEMS

This section gives thermal conductivity results for three periodic composites with two-dimensional lattices. The lattices are the square lattice the hexagonal lattice, and what we will call here the ''2D opal lattice.'' The square and hexagonal lattices are shown by the insets in Fig. 1 and are named for the geometries of their unit cells. They consist of nonoverlapping nonconducting cylindrical voids (in white) in a material characterized by κ_o (in gray). A 2D opal lattice is formed by an array of overlapping cylinders as shown in the inset of Fig. 2. The nonconducting star-shaped pores (in white) extend through a material characterized by κ_o (in gray).

We give results as functions of the porosity of the lattice. The porosity p is the fraction of the total volume occupied by the void regions. The lattice constants are the lengths of the vectors in Figs. 1 and 2. The square and hexagonal lattices exist only when the radii of the voids are less than half of the lattice constant. In the 2D opal the gray cylinders in Fig. 2 overlap. The upper limit of the porosity range is set when the cylninders no longer overlap.

All three two-dimensional lattices are characterized by circular or piecewise circular boundaries between materials. To solve for σ the boundaries were discretized using arc segments. For the square and hexagonal lattices the boundaries of the cylinders were broken into 200 discrete boundary elements each with constant σ. Similarly, the boundaries of the 2D opal were discretized uniformly with arc segments. Near the cusps of the 2D opal boundaries additional mesh points were necessary bringing the total to 320. The necessity of additional mesh points near cusps has been discussed previously in connection with isolated nanostructure calculations.[10,11] The present technique based on Eq. (8), which employs discretization of a boundary integral is considerably more efficient than finite-element or finite-difference techniques which require meshes over the entire area of the two-dimensional cell. Further, the lattice-periodic Green's functions satisfy all periodicity constraints in a natural way. Therefore the matrices obtained using $\tilde{g}$ are smaller than those obtained using g because using $\tilde{g}$ eliminates meshing the unit cell boundaries and imposing the periodic boundary conditions separately. The effective thermal conductivities were calculated using Eq. (10) in which the integral was evaluated by dividing the unit cell into a uniform grid. The resulting conductivities are for thermal current flow in the plane of the lattices.

The calculated thermal conductivities of the square and the hexagonal lattices are given by the solid lines in Fig. 1. The conductivities of these two-dimensional lattices go to zero when the conducting regions become disconnected. This occurs for different nonzero porosities in the two cases. The thermal conductivity given by the simple Maxwell-Garnett result from Eq. (1) (with $d=2$) is shown by the dotted line in Fig. 1. This model does not distinguish between the two lattices because it treats the inhomogeneities in only an average sense. The model results agree well with the present results for low porosities. This is as expected and it has been seen in another context.[15] For larger porosities they no longer agree well. Also the model fails to represent the disappearance of the thermal conductivity at $p<1$ when the systems break up into disconnected parts.

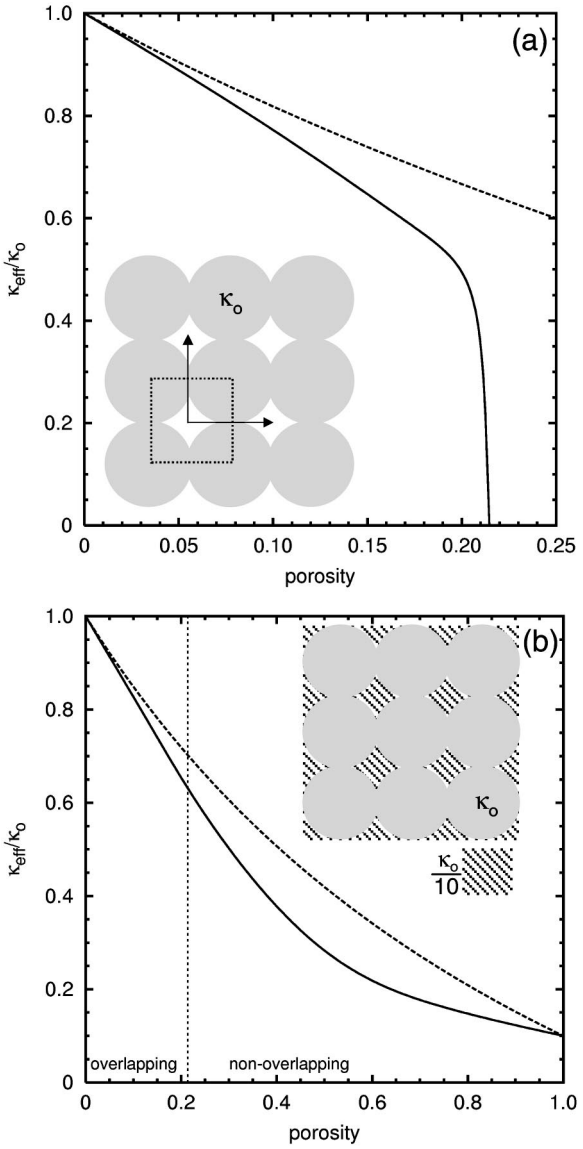

FIG. 2. Thermal conductivity vs porosity for the 2D opal lattice. The dashed curves are the Maxwell model results. The geometry of the 2D opal lattice defined by overlapping cylinders is pictured. (a) Case when the pores are not filled. (b) Case when the pores are filled with a material that has a different conductivity.

The calculated thermal conductivities of the 2D opal lattice is given by the solid line in Fig. 2(a). The conductivity vanishes at $p=0.214$ when the conducting regions cease to overlap. The Maxwell-Garnett result is shown again by the dotted line in Fig. 2(a). Clearly this simple model is an inadequate description of the conductivity of the 2D opal lattice for varying porosities. The effects of lattice geometry on

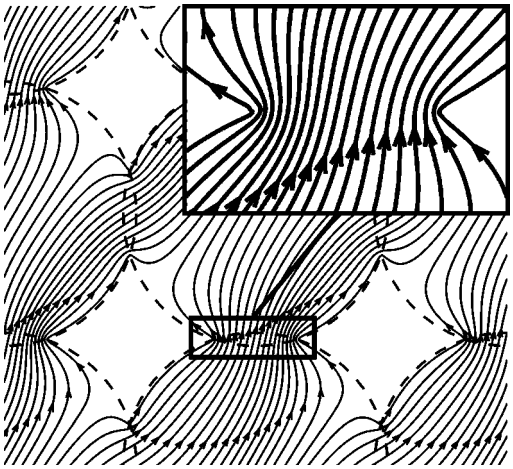

FIG. 3. A thermal flow pattern through a 2D opal lattice. The dashed circles give the geometry. Here the thermal field was applied at 60° from horizontal.

the composite conductivity are made obvious by comparing the resulting conductivities shown in Figs. 1 and 2(a). An additional system of interest is formed by filling the 2D opal intersticies with a material having a different thermal conductivity as shown in Fig. 2(b). For small or large porosities the thermal conductivity approaches that of the two constituent materials. The largest deviations from the simple model occur at intermediate porosities. Overall the 2D opal lattice impedes heat flow more effectively than the square and hexagonal lattices at comparable porosities. The stronger porosity dependence of the thermal conductivity for the 2D opal lattice is a geometrical effect.

A plot of the calculated current flow pattern for a 2D opal lattice is given in Fig. 3. The external field has been applied along a low-symmetry direction to demonstrate the flexibility of the boundary-element technique. An example of the current constriction in the 2D opal lattice is shown in the enlarged portion of Fig. 3.

The 2D opal lattice can serve as a guideline structure to demonstrate the modifications of thermal conductivity that can be caused by lattice geometry. The present calculations provide a starting point for understanding the porosity dependence of the thermal conductivity for a wider class of mesoscopic composites including those without periodicity.

IV. THREE-DIMENSIONAL SYSTEMS

This section gives thermal conductivity results for three periodic composites with three-dimensional lattices. The lattices are the simple cubic lattice, the fcc opal lattice, and the inverse-opal lattice. The simple cubic lattice consists of nonconducting spherical voids imbedded in a material characterized by κ_o. The simple cubic lattice is the three-dimensional analog of the two-dimensional square lattice but there is a key difference: it forms a lattice even when the spherical voids overlap. Therefore the porosity of the simple cubic structure can be broken into two regimes corresponding to spherical voids completely confined to their unit cells (nonoverlapping) and to spherical voids that overlap with the nearest neighbors (overlapping). As the void size is increased the lattice becomes ill defined when the radius of the void exceeds the lattice period divided by $\sqrt{2}$.

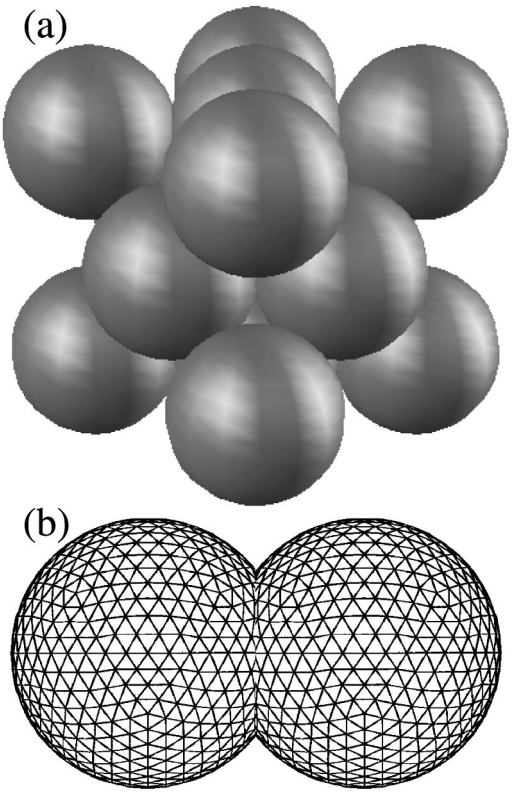

FIG. 4. (a) Face-centered-cubic opal lattice structure composed of overlapping spheres. (b) Schematic boundary-element meshing of overlapping spheres.

The fcc opal lattice is formed by an array of overlapping spheres arranged as shown in Fig. 4(a). The spheres have thermal conductivity κ_o and the remaining pores are nonconducting. The porosity limit of the fcc opal is reached when the 12 nearest-neighbor spheres no longer intersect. A difference between the 2D opal and the fcc opal is that the voids of the 2D opal are isolated whereas the voids of the fcc opal form a connected lattice. By reversing the roles of the spheres and voids in Fig. 4(a) we obtain an inverse-opal lattice which is a structure where the material inside the spheres has thermal conductivity κ_{pores} and the filled region κ_o. Examples of fcc opal and inverse-opal lattices can be found in Refs. 1 and 2. The porosity of the inverse opal is found by subtracting the porosity of its template opal from 1.

Calculations on the boundaries of these three-dimensional lattices involve discretizing spherical surfaces. To solve for σ the boundaries were discretized using equilateral geodesic triangles. The boundary-elements were taken to have piecewise-constant σ similar to the discretization used for two-dimensional lattices. Figure 4(b) gives a flavor of the essential meshing features showing both the surface triangles and the intersection of spheres. In more detail the mesh has 1280 boundary elements on a complete sphere for the nonoverlapping porosity regime of the simple cubic lattice and increased meshing near intersections of spheres for the overlapping simple cubic case as well as the fcc opal and inverse

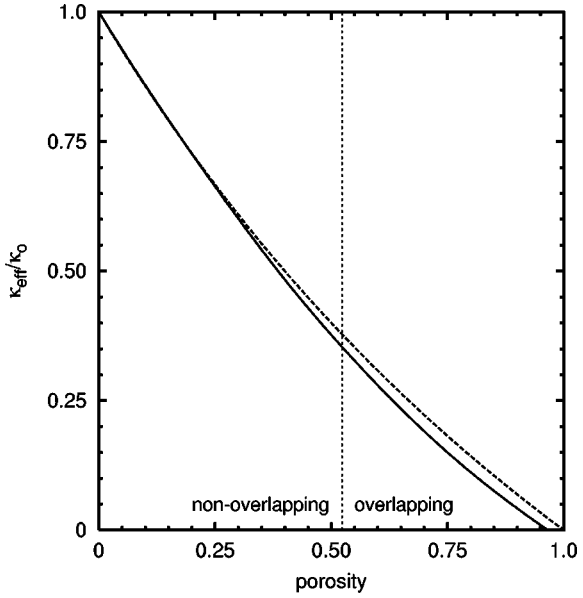

FIG. 5. Thermal conductivity as a function of porosity for the simple cubic lattice. The dashed curve is the Maxwell model.

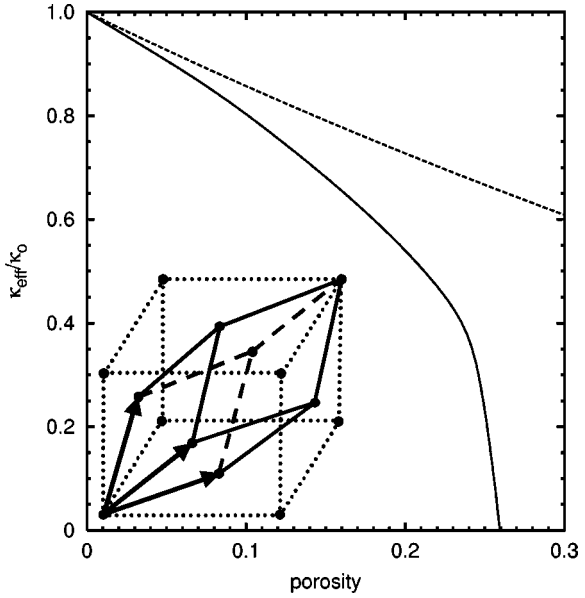

FIG. 6. Thermal conductivity of the fcc opal lattice vs porosity. The dashed curve is the Maxwell model.

opals. The number of mesh points is increased near the intersections of spheres by breaking the triangles into smaller equilateral triangles. Giraldo's technique of meshing spheres with uniform geodesic polygons, descriptions of triangle breaking, and pictures of the basic mesh are given in Ref. 16.

Meshing the boundary surfaces of these three-dimesional systems results in smaller matrices than implementations using volume finite elements. Our use of lattice-periodic Green's functions to eliminate boundary elements on the cell borders offers substantial numerical advantages for three-dimensional lattices because the unit-cell boundary is not discretized. The effective thermal conductivities were calculated using Eq. (10) and the integral was evaluated by dividing the unit cell into a uniform cubic grid. As a check the effective conductivities were obtained independently by calculating the ratio of the net heat flux through the unit-cell surfaces to the heat flux through an identical unit cell of isotropic material with conductivity κ_o.

The calculated thermal conductivity of the simple cubic lattice is given by the solid curve in Fig. 5. The nonoverlapping and overlapping geometry regimes are separated with a vertical line to indicate the crossover porosity. The Maxwell thermal conductivity shown by the dashed curve, is a good approximation to the simple cubic lattice for low porosity. As expected the thermal conductivity deviates from the Maxwell model as the porosity is increased but the trend is similar.

The calculated thermal conductivity for the fcc opal lattice is given by the solid curve in Fig. 6. The Maxwell result is shown for comparison. The conductivity of the opal vanishes for $p=0.259$ where the spheres shown in Fig. 4(a) no longer overlap. This feature is not represented well by the simple Maxwell model. Compared with the results for the simple cubic structure given in Fig. 5 the fcc opal geometry impedes the heat flow more than the simple cubic lattice at the same porosities.

The results shown in Fig. 7 as solid curves correspond to inverse opals with $\kappa_{pores}/\kappa_o=0$, $\frac{1}{4}$ and $\frac{1}{2}$. Note the different shape of the conductivity vs porosity curve for the inverse-opal lattice shown in Fig. 7 for $\kappa_{pores}/\kappa_o=0$ compared with the opal lattice in Fig. 6. The reason is that the inverse-opal lattice is well defined for porosities smaller than the smallest porosity that can be obtained by filling an opal template. Therefore if such lattices could be fabricated the conductivity would continue to increase with decreasing porosity. This situation is similar to the simple cubic lattice transition from overlapping to nonoverlapping spherical voids except the

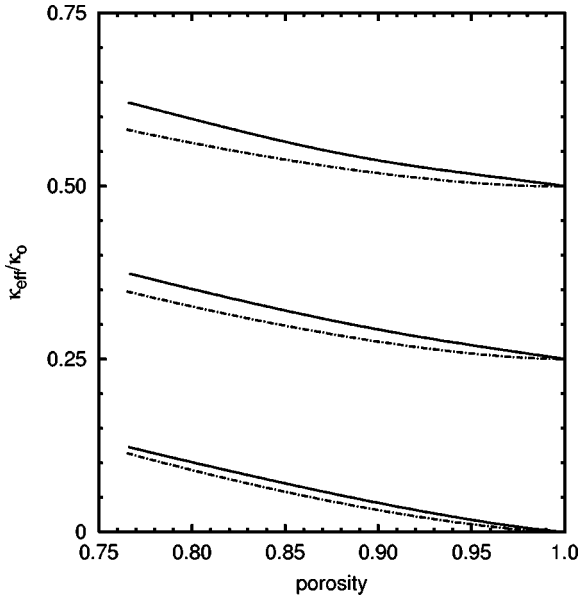

FIG. 7. Thermal conductivity of inverse-opal lattices. Results are given for $\kappa_{pores}/\kappa_o=0$ (lowest curves), $\frac{1}{4}$ (middle curves) and $\frac{1}{2}$ (top curves). The solid curves are our calculated results and the chain curves are after Bogomolov *et al.*

structure is face-centered cubic instead of simple cubic. The gains in conductivity from refilling the fcc opal are substantial as shown in the curves of Fig. 7 for κ_{pores}/κ_o equal to $\frac{1}{4}$ and $\frac{1}{2}$. In addition, the fcc opal and inverse-opal lattices can be filled with exotic thermoelectric materials giving a range of thermoelectric composites with low thermal conductivities.

A series of thermal conductivity and thermoelectric measurements have been published by Bogomolov *et al*. for the fcc opal and inverse-opal lattices.[17–20] Experiments[20] showed that the thermal conductivity of the inverse opals can be described roughly by an emperical model[21] given by $\kappa_{eff}/\kappa_o=(1-p)^{3/2}+p^{1/4}(\kappa_{pores}/\kappa_o)$. Comparing this expression (plotted with chain curves in Fig. 7) with our results (shown by solid curves) shows that the experimental fit is consistently lower than our calculations. That the two results agree as well as they do is surprising because the fabrication of inverse opals typically suffers from incomplete filling and flaws in the opal template.

V. CONCLUSION

Overall we have presented a general formalism for calculating the thermal conductivity of periodic composites using a continuum approach. The extension of highly efficient boundary-integral techniques through the use of cell-periodic Green's functions was given in some detail. The real-space methods we have described here can be extended to a variety of phenomena in mesoscopic composites such the harmonic electromagnetic wave behavior.

Here we have used a continuum approach to study the effective thermal conductivity of periodic composites with a number of two-dimensional and three-dimensional lattices. We have used these results to evaluate the applicability of the Maxwell conductivity model for porous composites. At low porosities the calculated effective thermal conductivities of the square and hexagonal two-dimensional lattices and of the simple cubic lattice are in good agreement with the Maxwell model for porous media. Our calculations show that geometrical effects can give rise to significant modifications of the porosity dependence of the thermal conductivity.

The boundary-integral fomalism we gave in Sec. II allows the investigation of lattices involving overlapping cylindrical and spherical geometries. We have given a theoretical treatment of the thermal conductivity of opal-class structures with both two- and three-dimensional lattices. In particular, results have been given for 2D opal, fcc opal, and inverse-opal lattices. We find that the opal geometries impede the flow of heat more strongly than nonoverlapping structures of comparable porosity. Furthermore, we have shown that by using the fcc opal and inverse-opal lattices as templates for filling with other materials increases and decreases in the net conductivity can be obtained.

It might be noted that within a continuum approach the electrical conductivity of these mesoscopic systems can be calculated in formally the same way as done for the thermal conductivity here. Roughly speaking the thermoelectric figure of merit is controlled by the ratio of the electrical conductivity to the thermal conductivity. If the boundary conditions on the electrical and thermal conductivities are similar then their ratio will not be affected by microstructuring in the form of a composite. Microscopic effects that can give rise to interface thermal resistances for thermal conductivities have been discussed recently,[6] however, and they can affect this ratio.

ACKNOWLEDGMENTS

J.D.A. was supported by the Naval Research Laboratory/National Research Council. This work was supported in part by the U.S. Office of Naval Research. J.D.A. thanks L. R. Ram-Mohan for helpful discussions.

[1] A.A. Zakhidov, R.H. Baughman, Z. Iqbal, C. Cui, I. Kharyrullin, S.O. Dantas, J. Marti, and V.G. Ralchenko, Science **282**, 897 (1998).

[2] C. López, A. Blanco, H. Míguez, and F. Meseguer, Opt. Mater. **13**, 187 (1999).

[3] For this noncrystalline material at low temperature the thermal phonon mean free path λ was estimated from the lattice thermal conductivity κ_{ph}, the volumetric heat capacity c_v, and the average sound velocity $\overline{u}$ using $\kappa_{ph}=\frac{1}{3}c_v\overline{u}\lambda$ using common values for silica.

[4] At room temperature the nonlinear acoustic phonon dispersions must be taken into account and we follow the method in P. Hyldgaard and G.D. Mahan, *Thermal Conductivity 23* (Technomic Publishing Co., Inc., Lancaster, PA, 1996), p. 172. The needed parameters were obtained from Landolt-Börnstein, *Numerical Data and Functional Relationships in Science and Technology*, edited by O. Madelung, New Series, Group *III*, Vol. 17, Pt. f (Springer-Verlag, Berlin, 1983); G.V. Samsonov, *Handbook of the Physicochemical Properties of the Elements* (IFI-Plenum, New York, 1968); Y.S. Touloukian and E. H. Buyco, *Specific Heat: Metallic Elements and Alloys, Thermophysical Properties of Matter: The TPRC Data Series*, edited by Y.S. Touloukian (IFI/Plenum, New York, 1970), Vol. 4, p. 23; D.N. Parkinson and J.E. Quarrington, Proc. R. Soc. London, Ser. A **67**, 569 (1954); Yu. I. Ravich, B.A. Efimova, and I.A. Smirnov, *Methods of Semiconductor Investigation as Applied to the Lead Chalcogenides PbTe, PbSe, and PbS* (Nauka, Moscow, 1968).

[5] E.T. Swartz and R.O. Pohl, Appl. Phys. Lett. **51**, 2200 (1987).

[6] S. Pettersson and G.D. Mahan, Phys. Rev. B **42**, 7386 (1990).

[7] J.C. Maxwell, *A Treatise on Electricity and Magnetism* (Dover, New York, 1954), pp. 435–441.

[8] D.J. Bergman and L.G. Fel, J. Appl. Phys. **85**, 8205 (1999); D.J. Bergman and O. Levy, *ibid.* **70**, 6821 (1991).

[9] J.O. Sofo and G.D. Mahan, Phys. Rev. B **62**, 2780 (2000).

[10] P.A. Knipp and T.L. Reinecke, Phys. Rev. B **45**, 9091 (1992).

[11] P.A. Knipp and T.L. Reinecke, Phys. Rev. B **54**, 1880 (1996).

[12] P.A. Knipp and T.L. Reinecke, Physica E (Amsterdam) **2**, 920 (1998).

[13] P.P. Ewald, Ann. Phys. (Leipzig) **64**, 253 (1921) [translated by A. Cornell, Atomics International Library, 1964]; C. Kittel, *Introduction to Solid State Physics*, 2nd ed. (John Wiley & Sons, New York, 1953), pp. 571–575.

[14] The simplification makes use of the special functions $E_1(x) = \int_x^\infty y^{-1} e^{-y} dy$ and $\mathrm{erfc}(x) = (2/\sqrt{\pi}) \int_x^\infty e^{-y^2} dy$.

[15] R. Tao, Z. Chen, and P. Sheng, Phys. Rev. B **41**, 2417 (1990).

[16] F.X. Giraldo, J. Comput. Phys. **136**, 197 (1997).

[17] L.I. Arutyunyan, V.N. Bogomolov, D.A. Kurdyukov, A.V. Prokof'ev, and I.A. Smirnov, Fiz. Tverd. Tela (St. Petersburg) **40**, 781 (1998) [Phys. Solid State **40**, 719 (1998)].

[18] V.N. Bogomolov, N.F. Kartenko, L.S. Parfen'eva, A.V. Prokof'ev, I.A. Smirnov, H. Misiorek, J. Mucha, and A. Jezowski, Fiz. Tverd. Tela (St. Petersburg) **40**, 573 (1998) [Phys. Solid State **40**, 528 (1998)].

[19] L.I. Arutyunyan, V.N. Bogomolov, N.F. Kartenko, D.A. Kurdyukov, V.V. Popov, A.V. Prokof'ev, I.A. Smirnov, and N.V. Sharenkova, Fiz. Tverd. Tela (St. Petersburg) **39**, 586 (1997) [Phys. Solid State **39**, 510 (1997)].

[20] V.N. Bogomolov, D.A. Kurdyukov, L.S. Parfen'eva, A.V. Prokof'ev, S.M. Smoilovich, and I.A. Smirnov, Fiz. Tverd. Tela (St. Petersburg) **39**, 392 (1997) [Phys. Solid State **39**, 341 (1997)].

[21] The expression used to fit the measured thermal conductivities of inverse-opal lattices was attributed in Ref. 20 to Litovskii [E.Ya. Litovskii, Izv. Akad. Nauk SSSR, Neorg. Mater. **16**, 559 (1980)].